TÜBİTAK

Turk J Elec Eng & Comp Sci, Vol.20, No.5, 2012, © TÜBİTAK
doi:10.3906/elk-1101-1056

Cascade fuzzy logic control of a single-link flexible-joint manipulator

İsmail Hakkı AKYÜZ*, Zafer BİNGÜL, Selçuk KİZİR
Department of Mechatronics Engineering, Faculty of Engineering, Kocaeli University, Umuttepe 41380, Kocaeli-TURKEY
e-mails: {ismail.akyuz, zaferb, selcuk.kizir}@kocaeli.edu.tr

Received: 24.01.2011

Abstract

This paper presents the design and control of a single-link flexible-joint robot manipulator. A cascade fuzzy logic controller (FLC) was used to remove link vibrations and to obtain fast trajectory tracking performance. The cascade FLC structure includes 3 different FLCs. The input variables of the first and the second FLCs are the motor rotation angle error, its derivative, and the end-point deflection error its derivative, respectively. The outputs of these controllers are the inputs of the third FLC, which yields the control signal to the flexible robot arm. All of the FLCs were embedded in a DS1103 real-time control board. Several experiments were conducted to verify the controller performance. In the step-response experiments, the error of motor rotation angle was obtained as less than 0.12° and there was no steady-state error in the end-point deflection. In trajectory tracking experiments with the same FLC structure, small errors and phase shifts in the system variables occurred. Model parameters of the flexible arm such as link length and spring stiffness were changed to test the robustness of the FLC. It was seen that the FLCs were very robust to internal and external disturbances. Considering the results of the experiments, the proposed FLC structure shows efficient control performance in flexible robot arms.

Key Words: *Fuzzy control, robot control, flexible manipulator*

1. Introduction

Flexibility in modern robot systems has become very important for satisfying the special needs of industrial automation and space systems. Control engineers have been working on the development of a mathematical model and the control of flexible structures. Flexible mechanisms and flexible-joint manipulators were applied for reducing the vibration in the remote manipulator system in a space station-assembly shuttle flight [1], performing decontamination tasks in nuclear maintenance and positioning the nozzle dam in the maintenance of a nuclear power plant's steam generator [2], remediating a waste storage tank [3], cleaning a waste tank [4], operating in microsurgical applications [5], positioning a patient system for cancer patient treatment [6],

*Corresponding author: Department of Mechatronics Engineering, Faculty of Engineering, Kocaeli University, Umuttepe 41380, Kocaeli-TURKEY

deburring [7], surface polishing [8], and grinding, painting, and drawing applications and biped-walking and walking machines [9]. They are mostly used in the service, space, medical, and defense industries.

Flexibility is generally an undesirable feature in robot manipulators because it causes significant control problems such as vibrations and static deflection. These control problems can result from external effects, designing errors, and the nonlinear dynamic behavior of flexible materials. The nonlinear vibrations decrease the end-point accuracy, increase settling time, and make the controller's design scheme complicated. However, special-purpose robot manipulators have been designed with flexible links that offer the following benefits: increased payload capacity (greater ratio of payload weight to robot weight), reduced weight of the arms (use of fewer powerful actuators), cheaper construction (fewer materials and smaller actuators), faster movements (faster accelerations because of lighter links), longer reach (more access and space because of a more slender construction), and safer operation (no damage because of the compliance and low inertia). According to a survey about flexible structures [10], the control algorithms developed for existing flexible systems have various limitations in terms of precision and accuracy. These features of the controllers could be improved using different control structures.

Two different control approaches to control flexible link mechanisms exist in the literature: linear control and nonlinear control methods. In the literature, the linear control methods developed for flexible robot manipulators are the linear quadratic regulator method [11], H_∞ control algorithms [12], proportional-integral-derivative (PID) control methods [13], and state feedback control [14]. It is quite difficult to control flexible mechanisms with conventional linear control methods due to the nonlinear dynamics of flexible structures and actuators. The nonlinear control methods applied to flexible robot manipulators in the literature are as follows: adaptive control schemes such as the adaptive neuro-fuzzy inference system (ANFIS) [15], the fuzzy model reference learning control (FMRLC) method [16], sliding mode control methods [17], the hybrid actuator scheme with a sliding mode controller [18], adaptive control using the sliding mode technique [19], PI-PD-PID-like fuzzy logic controllers [20], backstepping control design [21], and adaptive neural control [22].

The level of desired precision in flexible structures cannot be obtained with model-based control methods due to unmodeled nonlinear dynamics and unexpected external disturbances. Therefore, nonlinear methods that are not based on system models should be preferred in flexible mechanisms. In controlling nonlinear systems, the approach of fuzzy logic has found a distinguished position with its systematical capability of inclusion of human linguistic knowledge in the controller design [23]. Fuzzy logic controllers (FLCs) are widely used in many different control applications. Compared to conventional control algorithms with FLCs, sufficiently good results are obtained. There exist several advantages (no need for the mathematical model development) and disadvantages (difficulty in finding the optimum parameter) of this approach, as with all of the other control methods.

The studies related to FLCs and flexible systems in the literature can be summarized as follows. Khalil et al. [24] identified the parameters of flexible systems for performing sensorless motion control. Mougdal [25] developed an adaptive fuzzy controller to control a 2-link flexible manipulator. Passino et al. studied FMRLC for a 2-link flexible robot. Malki et al. [26] designed a fuzzy PID controller for a flexible-joint robot with uncertainties from time-varying loads. Lee et al. presented a FLC controller design for a flexible single-link manipulator. Subudhi et al. [27] proposed fuzzy and neuro-fuzzy approaches to control a flexible-joint robot. Mannani et al. [28] also developed a fuzzy Lyapunov synthesis-based controller for a 2-rigid link and 1-flexible link manipulator.

In this study, the vibration and trajectory tracking control of a flexible robot arm with FLCs are

developed for research purposes. The proposed FLC handles nonlinearity, flexibility, and uncertainty within the flexible-joint robot. Therefore, it produces remarkable positioning, tracking performance, and robustness. The organization of this paper is as follows. The solid model design of the flexible-joint robot and manufacturing of the arm are introduced in Section 2. Design of the FLC is explained in Section 3. Experimental results are discussed in Section 4. Finally, the conclusions are given.

2. Design and manufacturing of flexible-joint robot manipulator

In this work, the experimental setup of the flexible-joint robot was manufactured to study different control structures. The experimental setup consists of 2 main parts. The first main part is the servomotor (motor and encoder) and the second main part consists of a link, springs, and an encoder that is placed under the link (Figures 1,2,3). The encoder measures the link deflection. The experimental setup allows the use of 2 different link lengths (400 and 580 mm). Two springs are attached to both sides of the link (Figures 1,2,3). Spring stiffness constants were chosen as 5.468 N/m and 12.876 N/m. In order to reduce the total mass of the system, the material of the body was chosen as 6061 aluminum alloy sheet metal, 3 mm in thickness. Hence, the total mass of the robot arm (including the motor, gearbox, and encoder weights) was 2881.57 g. The motor and link parameters for the flexible joint are summarized in Table 1.

Table 1. Parameters of flexible-joint robot arm.

Symbol	Description	Value
R_m	Motor resistance	7.31 Ω
K_g	Gear ratio	66
K_m	Motor constant	0.0000783 N/(rad/s)
K_s	Spring stiffness	5.468 N/m
m	Link mass	0.0149 kg

The solid model, physical setup, and configuration of the flexible joint are shown in Figures 1, 2, and 3, respectively.

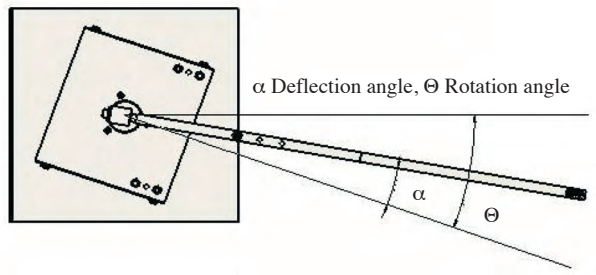

Figure 1. Configuration of the flexible-joint robot.

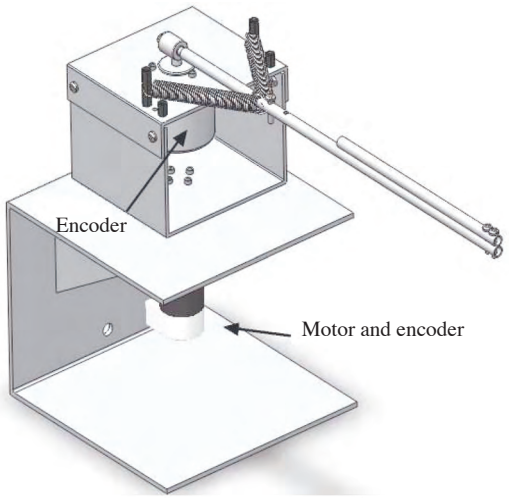

Figure 2. Solid model of the flexible arm.

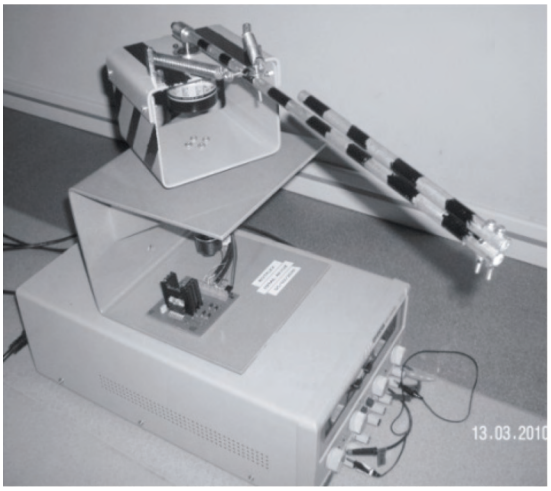

Figure 3. Experimental setup of the robot.

3. Design of fuzzy logic controller

In this section, the controller design of the flexible-joint robot arm is explained in detail. FLCs were implemented in the MATLAB® Fuzzy Logic Toolbox. Membership functions and rule bases were created in the Fuzzy Inference System Editor. Figure 4 shows a block diagram of the system and the structure of the cascade FLC. Each of the FLCs in this structure is responsible for different control tasks.

The inputs of the first and second FLCs (FLC-I and FLC-II) are the motor rotation angle error (θe) and the derivative of the rotation angle error $(\dot{\theta} e)$, and the deflection angle error (αe) and the derivative of the deflection angle error $(\dot{\alpha} e)$, respectively. The last controller takes the outputs of the first 2 controllers as inputs and yields the control signal of system (Figure 4). The third FLC (FLC-III) produces the necessary control signals for the motor driver.

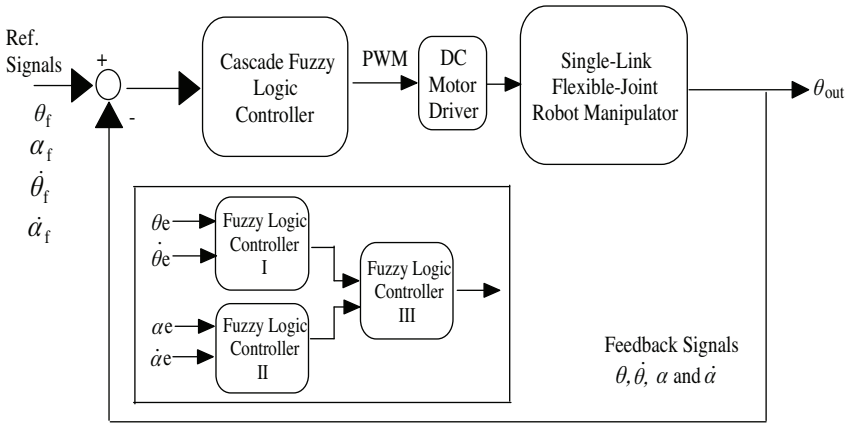

Figure 4. Block diagram of the system and structure of the cascade FLC.

The membership functions of FLC-I are illustrated in Figure 5. Inputs and the output of FLC-I are applied with a 9-triangle membership function [–4,–3,–2,–1,0,1,2,3,4]. Error of angle (θe) is scaled between -90° and $+90^\circ$. The error deviation of angle $(\dot{\theta} e)$ is scaled between -40° and $+40^\circ$ and the output function is

between –1° and 1°. The membership functions of FLC-II are shown in Figure 6. The inputs and the output of FLC-II are implemented with a 7-triangle membership function [–3,–2,–1,0,1,2,3], the error of angle (αe) is scaled between –30° and +30°, and the difference error of angle ($\dot{\alpha} e$) and the output of FLC-II is scaled between –1° and 1°. The membership functions of FLC-III are shown in Figure 7. The first input of FLC-III, the second input of FLC-III, and the output of FLC-III are applied with a 7-triangle membership function [–3,–2,–1,0,1,2,3], the first and the second input scales are between –0.87° and 0.87°, and the output function of FLC-III is scaled between –1° and 1°. The generated membership functions are illustrated in Figures 5-7.

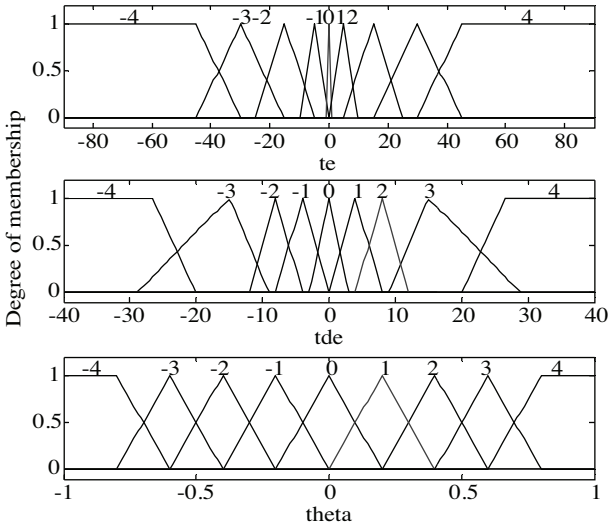

Figure 5. The membership functions of FLC-I for θ angle error, the derivative of θ angle error, and output.

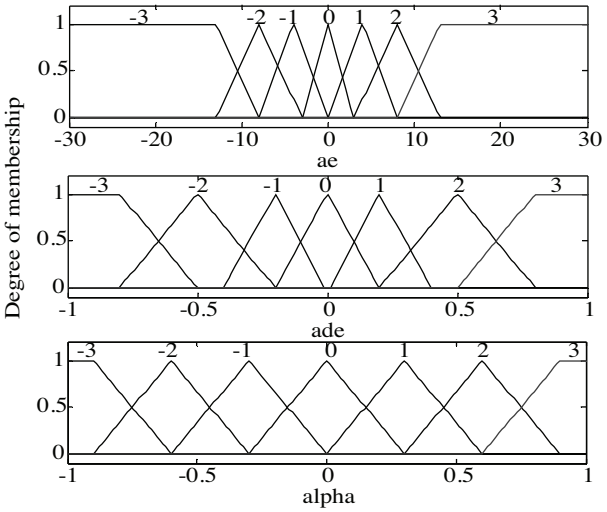

Figure 6. The membership functions of FLC-II for α angle error, the derivative of α angle error, and output.

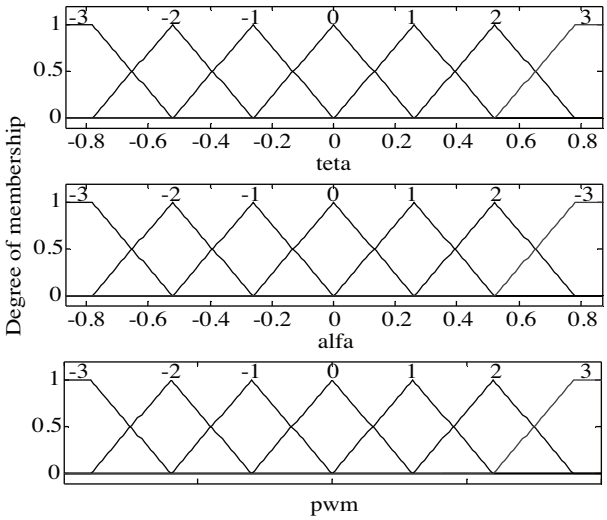

Figure 7. The membership functions for FLC-I output, FLC-II output, and FLC-III output.

After defining the membership functions, the rule tables for the FLCs of the flexible-joint manipulator are given in Tables 2-4, respectively. The first, second, and third FLCs have 81, 49, and 49 rules, respectively, in their rule bases.

Table 2. Rule table of FLC-I.

$\dot{e}$/e	−4	−3	−2	−1	0	1	2	3	4
−4	4	4	4	3	3	2	2	1	0
−3	4	4	3	2	3	2	1	0	−1
−2	4	3	3	2	2	1	0	−1	−2
−1	3	3	2	1	1	0	−1	−2	−2
0	3	2	2	1	0	−1	−2	−2	−3
1	2	2	1	0	−1	−1	−2	−3	−3
2	2	1	0	−1	−2	−2	−3	−3	−4
3	1	0	−1	−2	−3	−2	−3	−4	−4
4	0	−1	−2	−2	−3	−3	−4	−4	−4

Table 3. Rule table of FLC-II.

$\dot{e}$/e	−3	−2	−1	0	1	2	3
−3	3	3	2	2	1	1	0
−2	3	2	2	1	1	0	−1
−1	2	2	1	1	0	−1	−1
0	2	1	1	0	−1	−1	−2
1	1	1	0	−1	−1	−2	−2
2	1	0	−1	−1	−2	−2	−3
3	0	−1	−1	−2	−2	−3	−3

Table 4. Rule table of FLC-III.

α/θ	−3	−2	−1	0	1	2	3
−3	−3	−3	−3	−3	−2	−1	0
−2	−3	−3	−3	−2	−1	0	1
−1	−3	−3	−2	−1	0	1	2
0	−3	−2	−1	0	1	2	3
1	−2	−1	0	1	2	3	3
2	−1	0	1	2	3	3	3
3	0	1	2	3	3	3	3

In a FLC structure, min-max operators and the centroid purification method were used. The obtained control surfaces of the FLCs are illustrated in Figures 8-10, respectively.

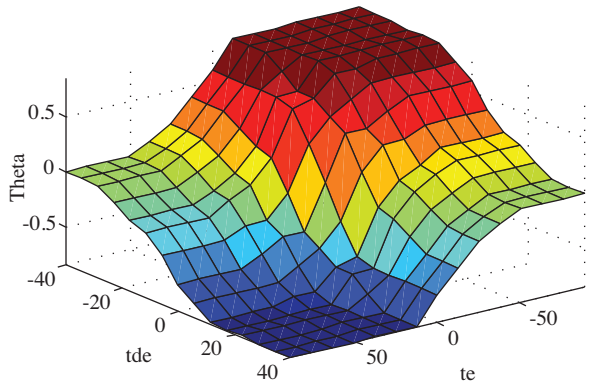

Figure 8. The control surface of FLC-I.

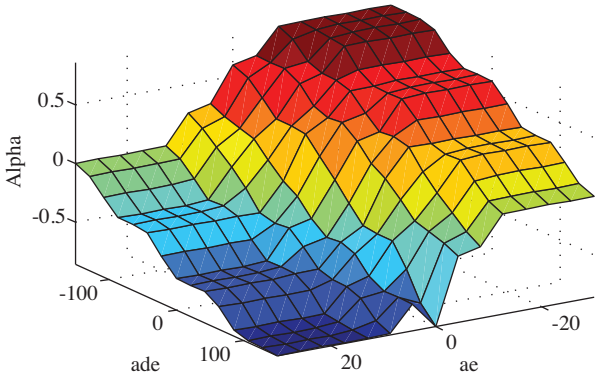

Figure 9. The control surface of FLC-II.

4. Results and discussion

The flexible arm has 4 major parts: the actuator, incremental encoders, the direct-current (DC) servomotor driver, and the controller with its computer interface. The actuator is a 24-V Maxon DC servomotor with 144 mNm of stall torque and 28.8 mNm of nominal torque. The servomotor is driven by an L-298 H-Bridge DC motor driver. It is equipped with a 0.12° resolution (500 counts/rev) incremental encoder to measure the rotation angle. The flexible joint is coupled to the DC servomotor with a planetary gearbox (66:1 reduction ratio

and average 0.3° backlash). This gearbox increases the measurement resolution to 0.011° (33,000 counts/rev) in the motor rotation angle. The second encoder measuring the end-point deflection angle has 0.12° resolution (500 counts/rev). The controller scheme was designed in Simulink® and embedded in the DS1103 control board.

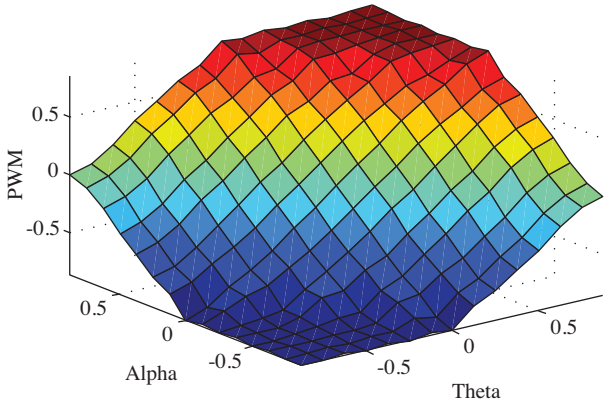

Figure 10. The control surface of FLC-III.

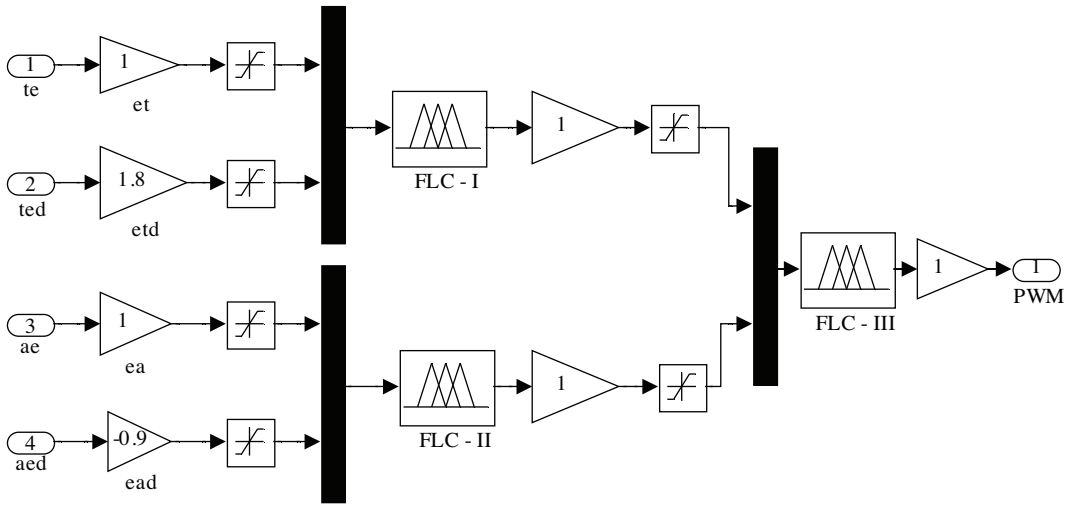

Figure 11. Cascade FLC structure in Simulink.

Simulink blocks of the main controller are shown in Figure 11. The controller includes 4 blocks: the measurement block, input block, output block, and controller block, as illustrated in Figure 12. The duty of the measurement block is to measure rotation and deflection angles, and the duty of the input block is to obtain the errors between reference and feedback signals. The output block produces the control signals and the control block yields the necessary pulse width modulation (PWM) signals for the DC servomotor driver.

To demonstrate the performance of the FLCs, a set of experiments was carried out on a single-link flexible-joint robot. The experiments can be grouped into 3 main parts: position control, trajectory tracking control, and robustness testing. To see the effect of each feedback signal on the system response, step functions were applied to the system. Figure 13 shows the step responses of the system for 3 different feedback signal mechanisms.

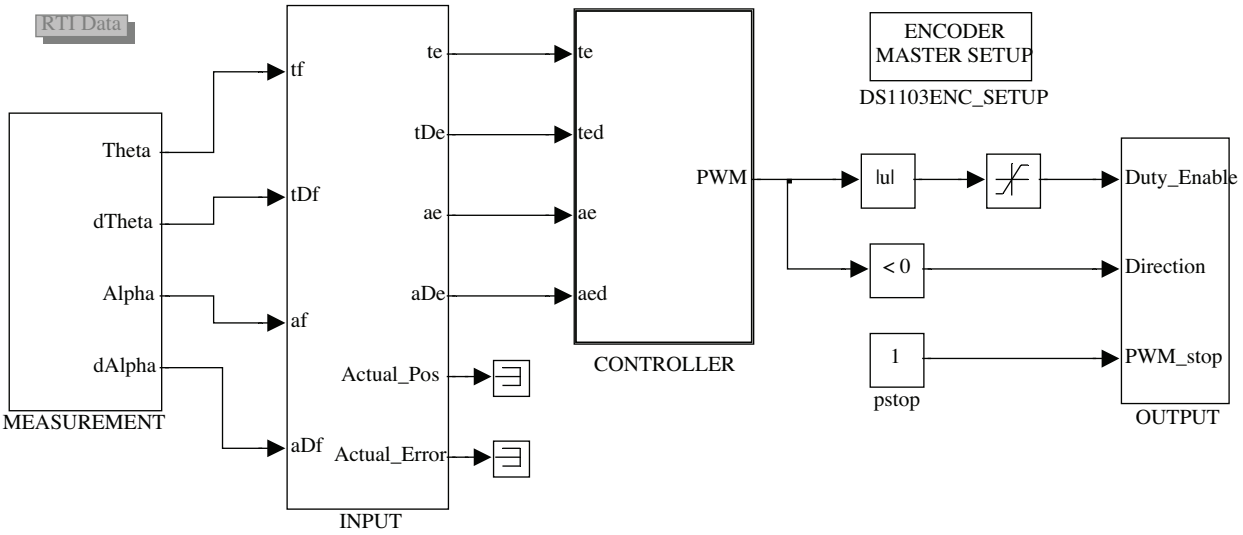

Figure 12. Main simulink model of the controller.

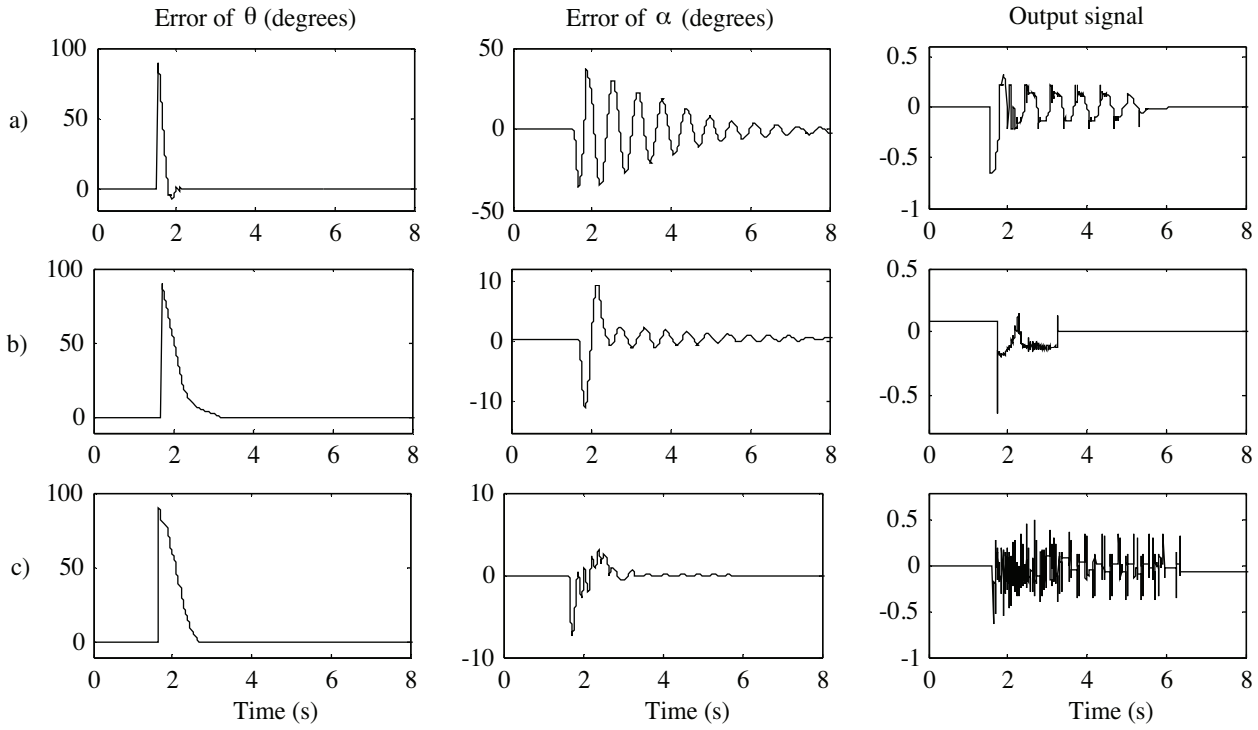

Figure 13. System step responses using different feedback signals.

First, only 1 feedback signal (θ) is used to control the system (Figure 13a); second, 2 signals (θ and $\dot{\theta}$) are feedback for the systems (Figure 13b); and finally, all of the feedback signals ($\theta, \dot{\theta}$, α, and $\dot{\alpha}$) are applied to the FLCs (Figure 13c).

As can be seen in Figure 13, the best response for the end-point deflection angle (reduced overshoot and vibration, and no steady-state error) was attained by using all of the state variables. However, the settling time

of the motor rotation angle was increased. As expected, more feedback signals produce more effective control. The comparison of the step responses of the FLCs is given in Table 5.

Table 5. Comparison of step responses obtained with different feedback signals.

Feedback signals	Motor rotation angle (θ)	End-point deflection angle (α)
Only θ	10° overshoot No steady-state error Faster rising and settling time than the others	Maximum 38° overshoot Slow decreasing oscillations
θ and $\dot{\theta}$	No overshoot Slower rising and settling time than the others	Maximum 10° overshoot Fast decreasing oscillations (less than 3°)
$(\theta, \dot{\theta},$ α and $\dot{\alpha}$	No overshoot Fast settling time No steady-state error	Maximum 7° overshoot Sharp decreasing oscillations (less than 1°) No steady-state error

In order to compare the control performance of the FLC and the PID controller, 2 serial PID controllers were applied to the joint (Figure 14). The first and second PID controllers control the θ and α angles, respectively. The constants of the PIDs for the θ and α angles are given in Table 6.

Table 6. PID constants for θ and α.

	PID I (θ)	PID II (α)
K_p	0.14	0.23
K_i	0.00002	0.00002
K_d	0.03	0.001

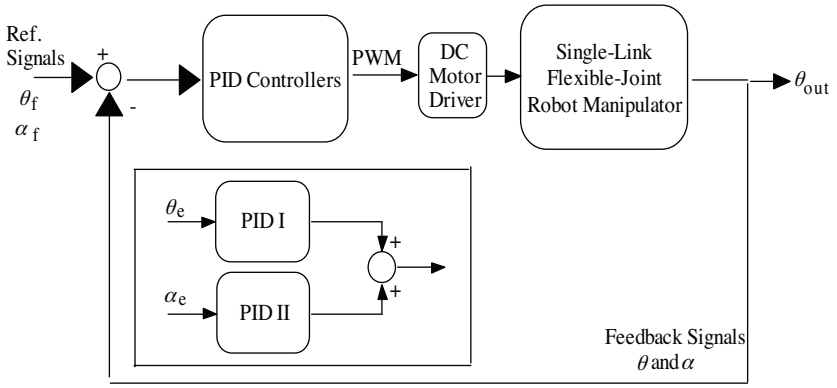

Figure 14. Block diagram of the system and PID controller structure.

Figure 15 illustrates the step response of the system for the PID controller. It can be seen that maximum 6° and 17° overshoots occurred at the θ and α angles, respectively.

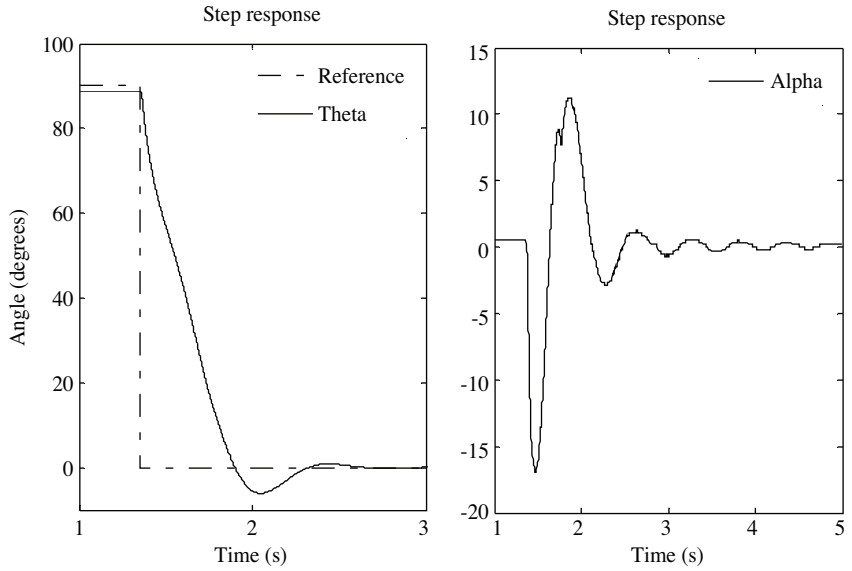

Figure 15. Step response of the PID controller.

Compared to the PID controllers, the FLC eliminates vibrations in a short time in the α angle and no overshoot occurs in the θ angle (Figure 13c). The developed FLC produces overall better results than the conventional PID controller in step-response experiments.

To see the system response in the case of external disturbances, external force impulses were applied to the end-point of the link. Figure 16 illustrates the input forces, the error of α angles, and the error of θ angles. As can be seen in Figure 16, the FLCs eliminate the external disturbances easily in 2 s.

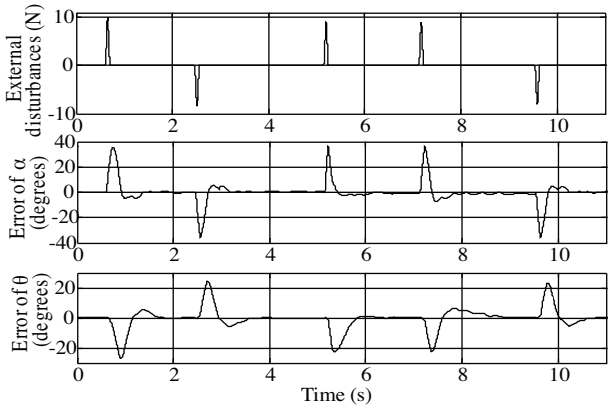

Figure 16. Response of the FLC with external input disturbances.

In the trajectory tracking experiments, 2 different trajectories were applied to the flexible joint to see the tracking performance of the FLC. The system responses for Kane and sinusoidal function trajectories are shown in Figures 17 and 18, respectively. In the Kane function trajectory tracking experiment, a maximum 0.4-s phase shift in the θ angle and maximum 1.62° vibrations in the α angle occurred. In the sinusoidal trajectory tracking experiment, the trajectory was tracked with no phase shift in the θ angle and 0.5° oscillations in the α angle. Considering the backlash of the planetary gearbox, the results obtained from the experiments are satisfactory.

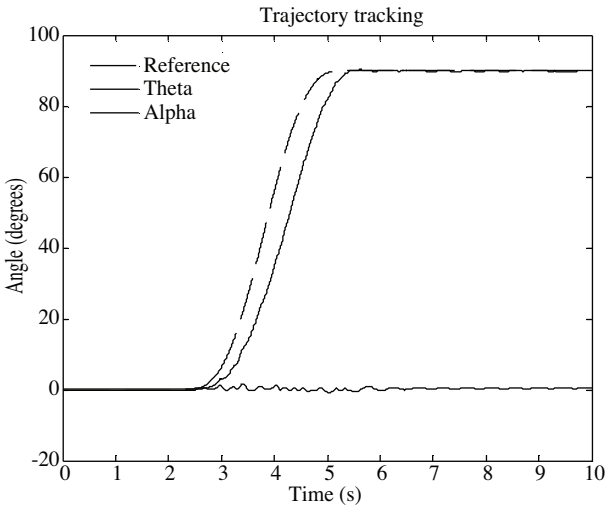

Figure 17. Responses for Kane trajectory tracking experiment.

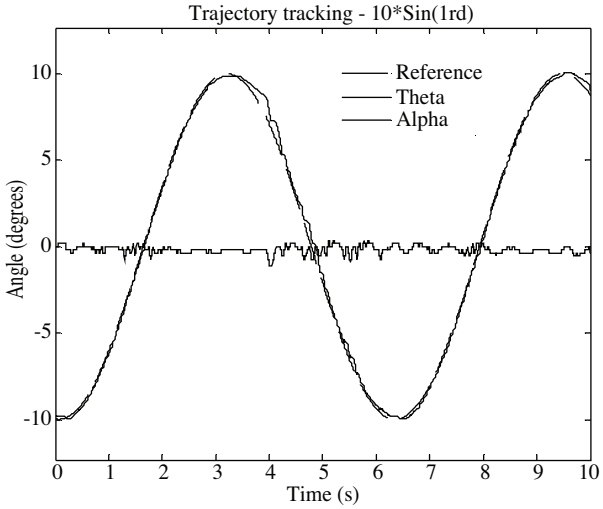

Figure 18. Responses for sinusoidal trajectory tracking experiment.

In order to test the robustness of the FLC, several experiments were conducted with 2 different link lengths and springs. Step input was applied to see the effects of longer link length on the performance of the FLC. The step response of the system with the longer link is shown in Figure. 19. As can be seen, the longer link makes system control difficult. As expected, the overshoot and settling time are increased and a steady-state error exists. Figure 20 illustrates the trajectory tracking behavior of the system with the longer link. Tracking errors (maximum of 1.5°), the phase shift in θ, and oscillations (maximum of 2.2°) in α are seen in Figure 20.

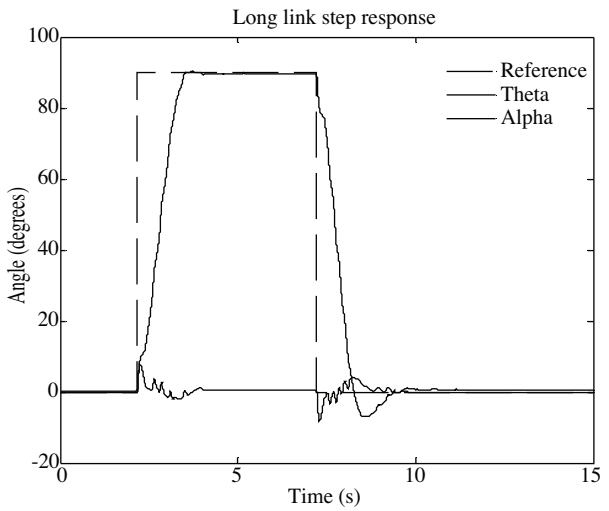

Figure 19. Step response for the longer link.

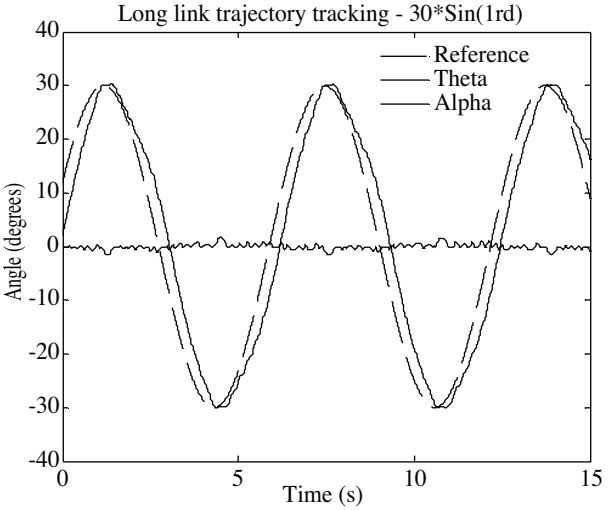

Figure 20. Trajectory tracking response for the longer link.

In order to see the stiffness effects of springs on the performance of the FLC, the spring was changed to a spring with a higher stiffness rate. The same experiments were repeated with this setup. Figure 21 illustrates the step response of the system with the FLC for a longer link and a stiffer spring. In the step-response experiment, the overshoot, settling time, and oscillations in the θ and α angles decreased. Figures 22 and 23

show the tracking performance of the FLC with a longer link and stiffer spring. Considering the results of all of the experiments, the best controller performance was achieved with the flexible arm with a shorter link and stiffer springs.

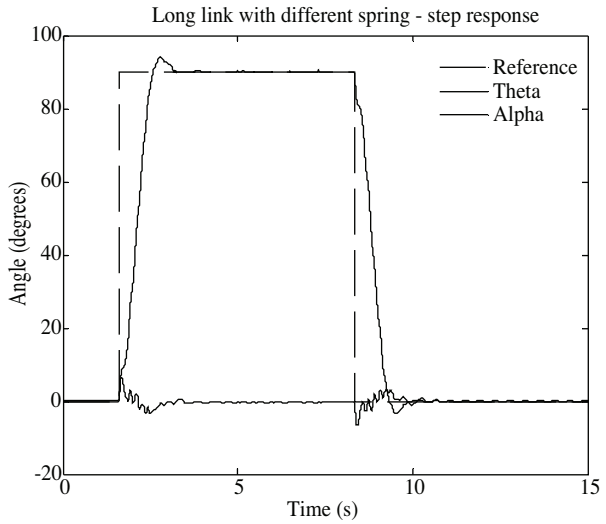

Figure 21. Step response for the longer link and stiffer springs.

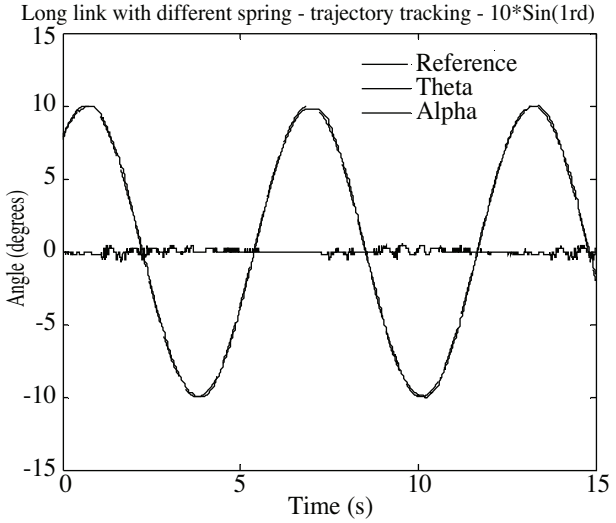

Figure 22. Sinusoidal function trajectory tracking of the longer link and stiffer springs.

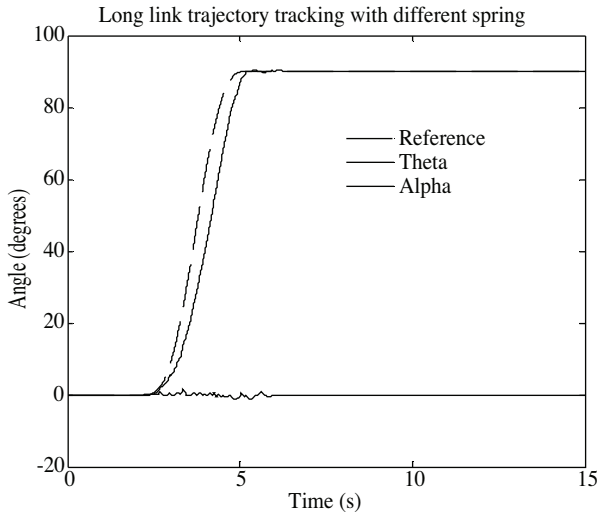

Figure 23. Kane function trajectory tracking of the longer link and stiffer springs.

5. Conclusion

In this study, positioning and trajectory tracking control of a single-link flexible-joint robot arm were implemented with a cascade FLC structure. Several step-response experiments were conducted to see the effect of different feedback signals on the response of the system. When the number of feedback signals in these experiments was increased, the vibrations of the end-point in the flexible joint decreased, as expected. In the position control experiments, no steady-state error was found and oscillations smaller than 0.5° were achieved in the

end-point of the link. In order to compare the performance of the cascade FLC with the PID controller, step inputs were applied to the system. Based on the comparison, the proposed FLC yields better results than the PID controller. In order to test the robustness of the proposed controller, external disturbances and changes in parameters such as link length and spring stiffness were employed. In the disturbance experiments, the cascade FLC structure was able to suppress link vibrations in a short time (maximum of 2 s). When a longer link was used, more overshoot and oscillations occurred in θ and α, respectively, and the performance of the trajectory tracking was reduced. As a stiffer spring was used, the vibration on the end-point was suppressed and the performance of the trajectory tracking was improved, as expected. Results of the robustness experiments show that the cascade FLCs are robust to external disturbances and system parameter changes. Due to the backlash of the planetary gearbox, a small phase shift occurred in the trajectory tracking experiments and a steady-state error of less than 0.2° occurred in the step-response experiments. Considering the results of all of the experiments, fast trajectory tracking and precise position control were obtained with cascade FLCs in the flexible-joint robot manipulators.

References

[1] S. Dubowsky, "Dealing with vibrations in the deployment structures of space robotic systems", Fifth International Conference on Adaptive Structures, 1994.

[2] M.A. Meggiolaro, S. Dubowsky, "Improving the positioning accuracy of powerful manipulators with application in nuclear maintenance", Proceedings of the 16th Brazilian Congress of Mechanical Engineering on Robotics and Control, pp. 210-219, 2001.

[3] J.F. Jansen, B.L. Burks, S.M. Babcock, R.L. Kress, W.R. Hamel, "Long-reach manipulator for waste storage tank remediation", Modeling and Control of Compliant and Rigid Motion Systems, Vol. 31, pp. 67-73, 1991.

[4] R. Kress, L. Love, R. Dubey, "Waste tank cleanup manipulator modeling and control", Proceedings of the IEEE International Conference on Robotics and Automation, Vol. 1, pp. 662-668, 1997.

[5] R. Kumar, P. Berkelman, P. Gupta, A. Barnes, P.S. Jensen, L.L. Whitcomb, R.H. Taylor, "Preliminary experiments in cooperative human/robot force control for robot assisted micro-surgical manipulation", Proceedings of the IEEE International Conference on Robotics and Automation, Vol. 1, pp. 610-617, 2000.

[6] M.A. Meggiolaro, S. Dubowsky, C. Mavroidis, "Error identification and compensation in large manipulators with application in cancer proton therapy", Revista Controle & Automacao, Vol. 15, pp. 71-77, 2004.

[7] I.C. Lin, L.C. Fu, "Adaptive hybrid force/position control of a flexible manipulator for automated deburring with online cutting trajectory modification", Proceedings of the IEEE International Conference on Robotics and Automation, Vol. 1, pp. 818-825, 1998.

[8] F. Pfeiffer, H. Bremer, J. Figueiredo, "Surface polishing with flexible link manipulator", European Journal of Mechanics A, Vol. 15, pp. 137-153, 1996.

[9] S. Gruber, W. Schiehlen, "Biped walking machines: a challenge to dynamics and mechatronics", Fifth World Congress on Computational Mechanics, 2002.

[10] W.J. Book, "Modeling, design and control of flexible link manipulator arms: a tutorial review", Proceedings of IEEE Conference on Decision and Control, pp. 500-506, 1990.

[11] R.H. Cannon, E. Schmitz Jr, "Initial experiments on the end-point control of a flexible one-link robot", International Journal of Robotics Research, Vol. 3, pp. 62-75, 1984.

[12] C. Trautman, D. Wang, "Experimental H_∞ control of a single flexible link with a shoulder joint", IEEE International Conference on Robotic and Automation, Vol. 1, pp. 1235-1241, 1995.

[13] M.T. Ho, Y.W. Tu, "PID controller design for a flexible-link manipulator", 44th IEEE Conference on Decision and Control, and European Control Conference, pp. 6841-6846, 2005.

[14] L.L. Tien, A.A. Schaffer, G. Hirzinger, "MIMO state feedback controller for a flexible joint robot with strong joint coupling", IEEE International Conference on Robotics and Automation, pp. 3824-3830, 2007.

[15] J.S.R. Jang, "ANFIS: Adaptive-network-based fuzzy inference systems", IEEE Transactions on Systems, Man and Cybernetics, Vol. 23, pp. 665-685, 1993.

[16] K.M. Passino, S. Yurkovich, "Fuzzy learning control for a flexible-link robot", IEEE Transactions on Fuzzy Systems, Vol. 3, pp. 199-210, 1995.

[17] Y. Kitamura, K. Iwabuchi, K. Nonami, H. Nishimura, "Positioning control of flexible arm using frequency-shaped sliding mode control", Third International Conference on Motion and Vibration Control, pp. 178-183, 1996.

[18] S.B. Choi, H.C. Shin, "A hybrid actuator scheme for robust position control of a flexible single-link manipulator", Journal of Robotic Systems, Vol. 13, pp. 359-370, 1996.

[19] R. Fareh, M. Saad, "Adaptive control for a single flexible link manipulator using sliding mode technique", IEEE 6th International Multi-Conference on Systems, Signals and Devices, pp. 1-6, 2009.

[20] M.N.H. Siddique, M.O. Tokhi, "GA-based neural fuzzy control of flexible-link manipulators", Journal of Engineering Letters, Vol. 13, pp. 148-157, 2006.

[21] J. Huang, J. Lin, "Backstepping control design of a single-link flexible robotic manipulator", Proceedings of the 17th World Congress of the International Federation of Automatic Control, pp. 11775-11780, 2008.

[22] A.R. Maouche, M. Attari, "Adaptive neural control of a rotating flexible manipulator", IEEE International Symposium on Power Electronics, Electrical Drives, Automation and Motion, pp. 517-522, 2008.

[23] J.X. Lee, G. Vukovich, "Fuzzy logic control of flexible link manipulators-controller design and experimental demonstrations", IEEE International Conference on Systems, Man and Cybernetics, Vol. 2, pp. 2002-2007, 1998.

[24] I.S.M. Khalil, E.D. Kunt, A. Sabanovic, "A novel algorithm for sensorless motion control of flexible structures", Turkish Journal of Electrical Engineering & Computer Sciences, Vol. 18, pp. 799-810, 2010.

[25] V.G. Mougdal, Direct, Supervisory, and Adaptive Fuzzy Logic Control of a Two-Link Flexible Manipulator, Master's Thesis, Department of Electric Engineering, The Ohio State University, 1993.

[26] H.A. Malki, D. Misir, D. Feigenspan, C. Guanrong, "Fuzzy PID control of a flexible-joint robot arm with uncertainties from time-varying loads", IEEE Transactions on Control Systems Technology, Vol. 5, pp. 371-378, 1997.

[27] B. Subudhi, A.S. Morris, "Fuzzy and neuro-fuzzy approaches to control a flexible single-link manipulator", Journal of Systems and Control Engineering, Vol. 217, pp. 387-399, 2003.

[28] A. Mannani, A., H.A. Talebi, "A fuzzy Lyapunov synthesis-based controller for a flexible manipulator: experimental results", IEEE Conference of Control Applications, pp. 606-611, 2005.